Photoinduced Generation of Long-Lived Proton Transfer States: Photoinduced Proton Transfer from 2-(2′,4′-Dinitrobenzyl)pyridine to a Proton Cage, the [2.1.1] Cryptand

K. Kuldová, A. Corval, and H. P. Trommsdorff*

Laboratoire de Spectrométrie Physique, Université J. Fourier Grenoble 1 - CNRS (UMR 5588), BP 87-38402 St Martin d'Hères Cedex, France

J. M. Lehn

Laboratoire de Chimie Supramoléculaire, Institut Le Bel, Université Louis Pasteur, 4 rue Blaise Pascal, 67000 Strasbourg, France

Received: April 21, 1997[⊗]

Photoinduced proton transfer from 2-(2′,4′-dinitrobenzyl)pyridine (α-DNBP) to [2.1.1] cryptand (C211) is demonstrated and characterized by transient absorption spectroscopy. Proton transfer is shown to occur from two tautomers reached after optical excitation of α-DNBP. Protonation of C211 is expected to form a proton cryptate in which the proton is included in the intramolecular cavity and stabilized, so that the back-transfer reaction is considerably slowed. As a consequence, the α-DNBP anion, formed by deprotonation, survives on time scales that are at least 10^3 times longer than those observed in the presence of another proton acceptor of similar basicity, triethylamine, which was studied for comparison and which does not equally stabilize the proton. As deprotonation by C211 intercepts different tautomers of α-DNBP, information about the reaction pathways of photocoloration in this compound is gained.

I. Introduction

Proton transfer (PT) from a donor to an acceptor can be photoinduced, if, after optical excitation, the donor becomes more acidic and if the rate of PT is high enough to compete efficiently with other decay channels of the excited state. In the electronic ground state the donor is reprotonated, making this process reversible. The PT is accompanied by a change of the electronic structure and spectra and may lead to significant color changes of the system. Such photochromic PT systems offer a number of attractive features for the design of molecular protonic devices and the development of light-controlled molecular functional units (e.g. photoactivated molecular switches).[1] An important issue of research in the area of molecular protonics[1] is the control of the efficiency of the various proton transfer reactions and of the relative stabilities and lifetimes of the different tautomers. Of particular interest is the photoinduced generation of long-lived proton transfer states, a process representing the protonic equivalent of the very actively studied photoinduced charge separation by electron transfer.

High efficiency requires that the rate of deprotonation of the proton donor site is fast as compared to the excited state lifetime, while the rate of back-transfer from the colored metastable tautomer should be slow. These seemingly contradictory requirements can be met by following a strategy where PT to a final acceptor site involves intermediate acceptor sites of lower acidity (or higher basicity) and higher stability. Sequential PT steps between these intermediates take place with lower rates than the initial deprotonation of the excited donor and often are accompanied or followed by structural changes which constitute barriers for the back-transfer to the original binding site of the proton. The optimization of the PT, regarding the stability of the phototautomer, is realized by a high ratio of the rates of forward- to back-transfer.

A way to increase the lifetime of a proton transfer state would be to introduce the proton into an intramolecular cavity so as to hinder the back-transfer. This is realized in proton cryptates, where the protons are concealed very efficiently and thus strongly shielded against deprotonation.[2,3]

SCHEME 1: Structure of the Macrobicyclic Cryptand C211 (left) and of Its Monoprotonated Proton Cryptate in the Endo−Endo Form (right)

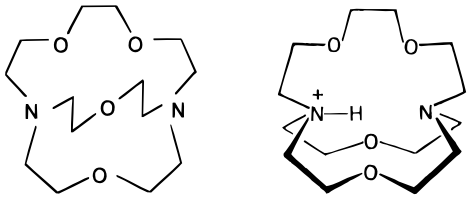

Here, we present a study aimed at exploring the use of [2.1.1] cryptand (C211, see Scheme 1), a so-called "proton cage", as a stabilized acceptor site of the proton in view of slowing down the back-transfer. Protonation of this cage may occur either externally or internally on a bridgehead nitrogen site oriented either out of (exo) or into (endo) the cavity, respectively. It is expected to lead eventually to the most stable monoprotonated species, a proton cryptate in which the proton is included in the intramolecular cavity and located on one of the nitrogen of the endo−endo form (Scheme 1). Internal protonation is accompanied by a structural relaxation which results in a pronounced shielding of the cryptated proton by the macrobicyclic cage which surrounds it tightly as shown by the crystal structure of the diprotonated [$2H^+$ 2.1.1] cryptate.[4] As a consequence, the deprotonation is markedly slowed, by a factor of about 10^7 with respect to the diffusion-controlled deprotonation of an unhindered ammonium site.[5] Ultimately it will be desirable to chemically link the photoactivated proton donor to the cage, so that this combined system may be incorporated in suitable host materials. However, to avoid demanding chemical synthesis of such linked systems in a first step and to validate the concepts proposed here, the present study is made in liquid solutions of mixtures of a photoactivated proton donor and C211 as proton acceptor. Since the reaction rate is limited by

[⊗] Abstract published in *Advance ACS Abstracts,* August 15, 1997.

S1089-5639(97)01363-7 CCC: $14.00

SCHEME 2: Light-Induced and Thermal Interconversions between Tautomers of 2-(2′,4′-Dinitrobenzyl)pyridine (α-DNBP)

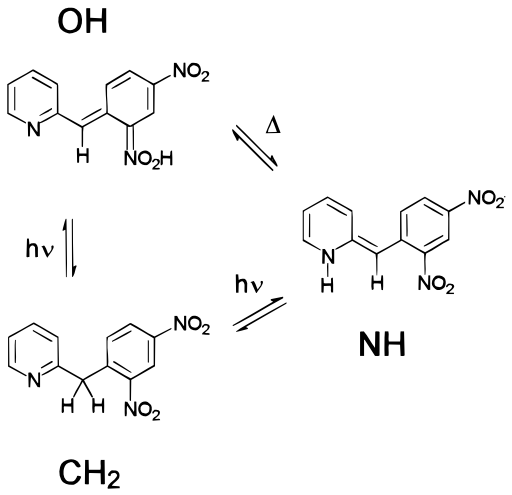

diffusion, the donor molecule, after electronic excitation, must reach a state of increased acidity that has a decay rate at least comparable to or smaller than the collision rate between the reaction partners to enable the transfer from the proton donor to the cage.

2-(2′,4′-Dinitrobenzyl)pyridine (α-DNBP) is a suitable candidate which, as shown here, fulfills these requirements. Indeed, α-DNBP itself exhibits photochromism resulting from an intramolecular PT from the methylene group to the nitrogen of the pyridine.[6−8] This reaction is observed, after optical excitation of the $S_0 \rightarrow S_1$ transition in the near-UV, in liquid solutions, in solid matrixes, as well as in pure crystals. Scheme 2 shows the mechanism that has been proposed for this proton transfer reaction.[9] In the electronic ground state the "CH_2" tautomer is the most stable form. Upon electronic excitation, the increase of the acidity of the CH_2 tautomer leads to a parallel as well as stepwise proton transfer which populates the "OH" and "NH" tautomers.[9−12] The NH tautomer, having the lowest acidity, is the more stable, finally populated form from which the back-transfer to the stable ground state CH_2 tautomer of α-DNBP takes place. The lifetime of the photogenerated metastable NH tautomer, which absorbs in the visible spectral region around 560 nm, is fairly long, ranging, at room temperature, from a few milliseconds in toluene solutions to a few hours in the pure crystal.

In fact, the proton transfer in α-DNBP, as shown in Scheme 2, realizes the first steps of a cascading PT. Measurements in the crystal show that the generation of the NH tautomer occurs by two different routes,[9,10] a fast PT process tentatively assigned to an excited state reaction and a slower process with a rate that is significantly lower than the fast deprotonation of the excited CH_2 tautomer. This ground state route involves as intermediates the OH tautomer and even shorter lived intermediates which are not shown in the simplified Scheme 2. The structural changes in these steps make the geometry less favorable for the back-transfer. Recent results indicate that an analogous scheme can be applied to the reactions identified in solution.[12]

Even though the validity of the concept of using C211 is demonstrated here with α-DNBP as proton donor, the concept is obviously quite general and could be implemented using other excited state proton donor molecules.

As expected and as born out in the present work, the acidity of α-DNBP, in the electronic ground state, is sufficiently low so that, even in the presence of a high excess of C211, the equilibrium is entirely displaced toward the stable CH_2 tautomer of α-DNBP. The present study also shows that the acidity of the electronically excited CH_2 tautomer as well as that of the OH and NH tautomers and possible intermediates is higher than the acidity of the protonated cage. PT to the cage is therefore possible from all these tautomer states, which are reached by and subsequent to electronic excitation. Since the rate of PT to the cage is diffusion controlled in liquid solutions, the transfer from the short-lived excited CH_2 tautomer to the cage is totally inefficient. As will be demonstrated here, PT to the cage becomes feasible from both longer lived OH and NH tautomers, and the rate of decay of the deprotonated α-DNBP anion is much smaller than rate of generating it, so that the α-DNBP−cryptand system exhibits indeed photochromism.

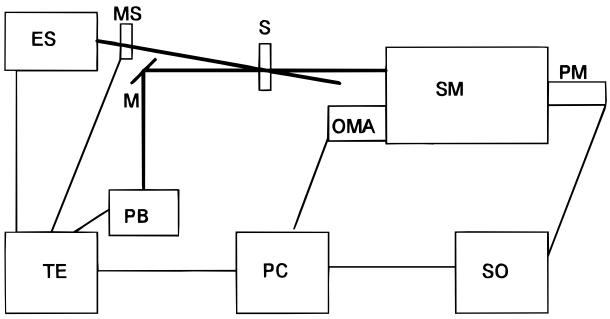

Figure 1. Setup used for transient spectroscopy: S, sample; ES, excitation source; PB, probe beam source; TE, timing electronics; SM, spectrometer; OMA, optical multichanel analyzer; PM, photomultiplier; SO, storage oscilloscope; PC, microcomputer; MS, mechanical shutter used to select single-laser pulses; M, mirror.

In the following, we present transient absorption measurements, made after pulsed laser excitation, of solutions of α-DNBP and the C211. For comparison, some measurements with triethylamine (TEA) as proton acceptor are also presented. The transfer to the proton acceptor (cage, TEA) is demonstrated via the observation of transient spectra which can be attributed to the deprotonated α-DNBP anion. Furthermore, the analysis of these transient spectra yields new information concerning the reaction intermediates involved in the photocoloration of α-DNBP itself and therefore gives new insights in the photochromic reaction of this compound.

II. Experimental Section

Sample Preparation. *Solvents.* All solvents used are "dry" solvents: toluene was distilled over appropriate drying agents under nitrogen atmosphere, and methanol and dichloromethane were kept over basic alumina for 24 h. Solvents were subsequently handled under exclusion of air and transferred to dried measurement cells.

Products. α-DNBP (Lancaster) was purified by recrystallization in ethanol and dissolved in dry toluene to eliminate traces of water. Toluene was removed by evaporation, yielding α-DNBP ready for use. C211, 4,7,13,18-tetraoxa-1,10-diazabicyclo[8.5.5]eicosane (98%) (Aldrich), was purified by chromatography over a basic alumina column, prepared in a dichloromethane/methanol mixture. The cage was dissolved in dichloromethane and eluted with methanol. The TEA was distilled and conserved on KOH.

Transient Spectra. Time-resolved measurements were made with the setup shown in Figure 1.

The excitation source is the third harmonic (355 nm) of a Nd:YAG laser (20 mJ pulse energy, 8 ns duration). The probe beam is a spectral quasi-continuum, delivered either by a pulsed Xe lamp (EGG FX 800, HighSpeedPhoto System Nanolite driver, ca. 300 ns duration) or by a continuous wave (CW) 50

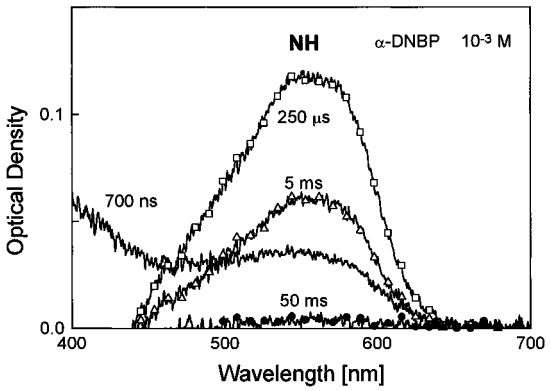

Figure 2. Transient absorption spectra of α-DNBP (1×10^{-3} M) in dry toluene at time delays after laser excitation as indicated. Below ca. 450 nm the spectra are distorted by solvent fluorescence.

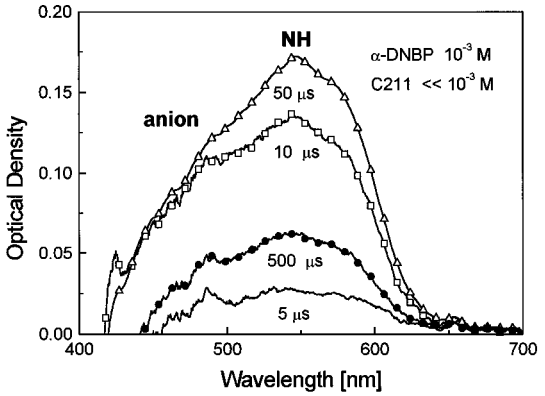

Figure 3. Transient absorption spectra of α-DNBP (1×10^{-3} M) with traces of cryptand C211 ($\ll 10^{-3}$ M) in dry toluene at time delays after laser excitation as indicated. Below ca. 450 nm the spectra are distorted by solvent fluorescence.

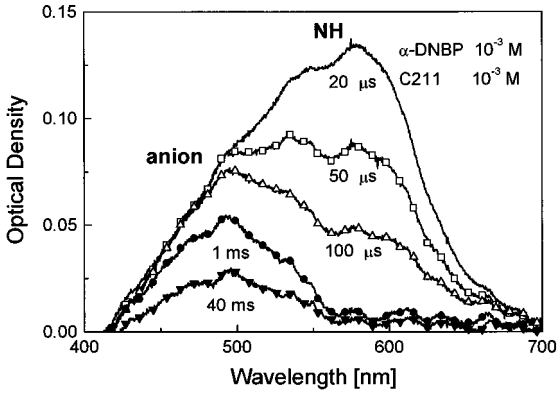

Figure 4. Transient absorption spectra of α-DNBP (1×10^{-3} M) with 1×10^{-3} M of cryptand C211 in dry toluene at time delays after laser excitation as indicated. Below ca. 450 nm the spectra are distorted by solvent fluorescence.

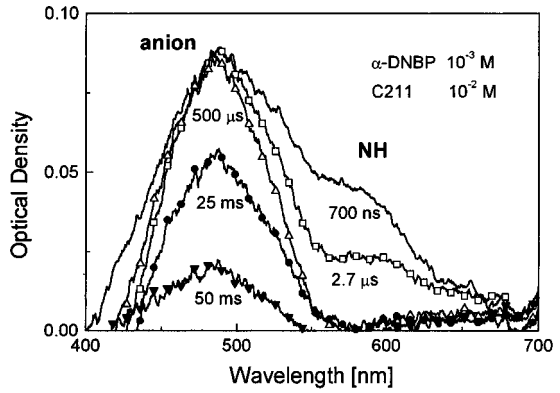

Figure 5. Transient absorption spectra of α-DNBP (1×10^{-3} M) with 1×10^{-2} M of cryptand C211 in dry toluene at time delays after laser excitation as indicated. Below ca. 450 nm the spectra are distorted by solvent fluorescence.

W tungsten lamp. The excitation beam is focused to a spot size of ca. 1 mm diameter. The optical path length of the sample cell is 1 cm. The excitation and the spatially filtered probe beams are crossed in the sample at an angle of about 10° in order to maximize the spatial overlap. The effective path length of the volume in which both beams overlap is ca. 0.25 cm. The setup enables the recording of transmission spectra, at variable delays between the excitation and pulsed probe light, over spectral intervals of 400−800 nm with a nominal resolution of 0.7 nm using a spectrometer (Chromex #500SH) with a grating of 150 grooves/mm, equipped with a cooled optical multichannel analyzer (OMA, Princeton Instruments ST130 LN/CCD). Alternatively, using the CW lamp as the probe beam source, the temporal evolution of the transmitted light is recorded with a photomultiplier tube (Hamamatsu R1546) and a storage oscilloscope.

The time scale in these experiments ranges from $\sim 10^{-7}$ to 10^{-2} s and is limited by the duration of the probe pulse at short times and, at long times, by the diffusion of the solute molecules out of the excited volume.

In the figures, spectra corresponding to the maximum optical density of the transient species are displayed together with representative spectra best illustrating the kinetics of these species.

Systematic Errors and Reproducibility. The solution phase reactions studied here extend to fairly long time scales and are therefore extremely sensitive to minute traces of impurities, which may catalyze these reactions. Impurities not only arise from traces of contaminants of the products used as well as residues of humidity but also are generated, as photodegradation products of the solute, by the optical excitation of the sample. Even though care was taken to use fresh samples in each experiment, these factors limit the reproducibility between different experiments to about a factor of 2, regarding the determination of time constants or reaction rates. Since, however, the effects investigated here lead to changes of these parameters by orders of magnitude, the results are only little affected by these fairly large systematic errors, which exceed by far the experimental measurement errors of less than 10%. Other sources of error which limit the data analysis at short times and, in particular, toward the short-wavelength region are stray laser light and fluorescence from the solvent.

III. Results and Assignments

Figures 2−5 show transient absorption spectra of pure α-DNBP (10^{-3} M) in dry toluene and in solutions with various amounts of C211 added. These spectra are the difference of spectra with and without laser excitation. The indication of negative optical densities, observed below ca. 450 nm, is not due to bleaching of the absorption of the sample, but results from the emission of the solvent that contributes to the signal even at longer probe pulse delays as the signal of the OMA is time integrated. In Figure 2, the short-lived absorption around 400 nm observed at a 700 ns delay is assigned to the OH tautomer. The NH tautomer absorbs at ∼560 nm and has a lifetime of about 8 ms. Addition of various amounts of C211 leads to marked changes of the transient spectra as detailed below and in particular to the observation of the α-DNBP anion as a new transient species. In contrast, the addition of C211, even at a high excess relative to α-DNBP, does not lead, in the

TABLE 1: Rise (↑) and Decay (↓) Rate Constants of the Three Transient Species Observed for Solutions of α-DNBP in Dry Toluene with Various Amounts of Cryptand C211 and/or TEA Added

concentrations [M]	OH	NH	anion[a]
$10^{-3}/0$[b]	↑ 10^6 s^{-1}	↑ 10^4-10^5 s^{-1}	not detected
(Figure 2)	↓ 2.10^5 s^{-1}	↓ 10^2 s^{-1}	
$10^{-3}/\ll 10^{-3}$ [b]	not detected	↑ 10^5 s^{-1}	not quantified
(traces, Figure 3)		↓ $(3 \pm 1) \times 10^3$ s^{-1}	
$10^{-3}/10^{-3}$ [b]	not detected	↑ 10^6 s^{-1}	↑ 10^6 s^{-1}
(Figure 4)		↓ 10^4 s^{-1}	↓ 3×10^3 s^{-1} OD^{-1}
$10^{-3}/10^{-2}$ [b]	not detected	↑ 10^6 s^{-1}	↑ 10^6 s^{-1}
(Figure 5)		↓ $(3.5 \pm 1.5) \times 10^5$ s^{-1}	↓ $(2.6 \pm 0.7) \times 10^2$ s^{-1} OD^{-1}
	not detected	↑ 10^6 s^{-1}	↑ 10^6 s^{-1}
$10^{-3}/10^{-3}$ [c] (Figure 6)		↓ $(1.9 \pm 0.7) \times 10^4$ s^{-1}	↓ not quantified

[a] The bimolecular rate constants describing the decay of the anion are given in units of [s^{-1} OD^{-1}] (see text). [b] α-DNBP/cage. [c] α-DNBP/TEA.

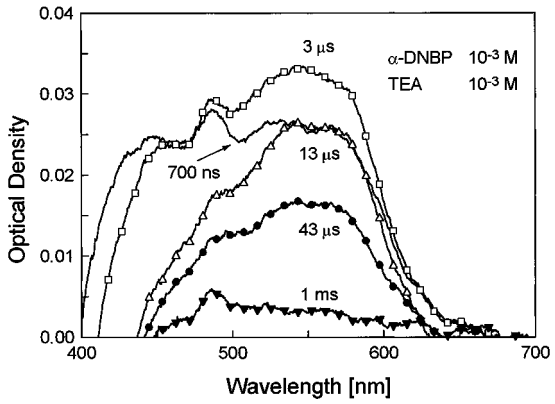

Figure 6. Transient absorption spectra of α-DNBP (1×10^{-3} M) with TEA (1×10^{-3} M) in dry toluene at time delays after laser excitation as indicated. Below ca. 450 nm the spectra are distorted by solvent fluorescence.

absorption spectra of unexcited solutions, to any observable spectral changes in the spectral region where the absorption of the transient species is monitored.

Figures 3−5 show transient spectra of solutions of 1×10^{-3} M α-DNBP in toluene with various amounts of C211 added. The main observations made from all of these spectra as well as from recordings of the time evolution at different wavelengths are collected in Table 1 and may be summarized as follows. The addition of the cage results in the following changes: (1) the disappearance of the OH tautomer at the time resolution of the experiment, (2) a shortening of the rise and decay times of the NH tautomer which parallels the increase of the concentration of C211, and (3) the appearance of a new transient absorption around 490 nm. The decay kinetics of this fairly long-lived absorption is discussed below and indicates a collisional process with a rate that is not diffusion, but reaction controlled.

The new transient absorption at 490 nm is assigned, by comparison with the spectrum of the chemically produced anion,[13] to the deprotonated anion of α-DNBP. The initially generated anion concentration becomes independent of the concentration of the cryptand when this concentration is at least equal to the concentration of α-DNBP. To establish that the rate of back-transfer, that is the decay of the α-DNBP anion, is limited by the escape of the proton from C211 and not by the small driving force due to a high basicity of the cage or other geometrical factors linked to α-DNBP, the effect of TEA was also investigated. TEA has a basicity comparable to that of the cage ($pK_a = 11.17$[5a]). Figure 6 shows transient spectra of toluene containing concentrations of α-DNBP and TEA equal to 1×10^{-3} M. The generation of the α-DNBP anion is clearly observed. However, while the effect of the addition of TEA on the kinetics of the OH and NH tautomers is comparable to the one observed upon addition of C211, the decay of the anion is faster by nearly 4 orders of magnitude.

The analysis of the kinetic behavior of the different species identified in the solutions is limited by the experimental uncertainties detailed above and also by the spectral overlap of the different species for which the extinction coefficients are known only with considerable uncertainty. The time evolution of the OH and the NH tautomers is expected to follow exponential laws, arising from feeding and decay processes that have both unimolecular as well as bimolecular contributions. The latter involve either impurities, catalyzing the reactions, or the proton acceptor molecules C211 and TEA present in large excess so that their population change can be neglected. The rise of the anion absorption follows the same law, while the decay is a bimolecular process involving equal populations of the two reacting species (anion and protonated C211 or TEA) and therefore follows a hyperbolic law:

$$c(t) = c(0)/(1 + c(0)k_B t) \qquad (1)$$

$c(t)$ is the concentration of the anion and k_B the bimolecular rate constant. The observed kinetics were found to be in agreement with these expectations, and the parameters listed in Table 1 were derived according to these. In equimolar 1×10^{-3} solutions of α-DNBP with C211, the evolution of the anion concentration shows, in addition to the fast ($>10^5$ s^{-1}) initial rise, a slower (10^4 s^{-1}) growth component, which parallels the NH decay. Under these conditions, the anion decay is described by a bimolecular kinetic equation with an exponential feeding term:

$$\mathrm{d}/\mathrm{d}t(c(t)) = -k_B c(t)^2 + c_{NH} \exp(-k_{NH} t) \qquad (2)$$

The initial concentration of NH is c_{NH}, and k_{NH} is the corresponding exponential decay constant (which equals the product of the quasi constant concentration of C211 and the bimolecular rate constant of PT from NH to the cryptand). Numerical integration of (2) shows that under the experimental conditions used the time scales of the feeding and decay contributions are sufficiently well separated, so that, except at early times, the decay of the anion concentration can, in these experiments, also be analyzed with (1). Because of the considerable uncertainty related to the molar extinction coefficient of the anion, ϵ_{AN}, and for better comparison between different experiments, the relative concentrations are measured in optical density (OD) units (at l cm path length) so that the bimolecular rate constants quoted in Table 1 have units of s^{-1} OD^{-1}, which can be converted to the conventional units of s^{-1} M^{-1} by multiplication with ($\epsilon_{AN} \times l$, with l in cm).

IV. Discussion

The experiments described above clearly demonstrate the occurrence of PT, after optical excitation, from α-DNBP to C211

(and TEA) with the concomitant generation of the α-DNBP anion. PT is shown to take place from both the OH and the NH tautomers. The collision rate with the cryptand at concentrations of 1×10^{-3} M lies in the range 10^6-10^7 s^{-1}. This rate is faster than the intrinsic decay rate of OH ($\approx 2.5 \times 10^5$ s^{-1}) measured in pure toluene solutions. The fact that even for about 10 times lower concentrations of C211 (and correspondingly lower collision rates) OH is quenched below the detection limit of our experiment indicates that PT from OH to the cage is diffusion controlled and not reaction rate limited.

The observation that NH is generated and can be detected even at cage concentrations of 1×10^{-2} M, proves that NH is not only produced via the decay of OH as demonstrated in previous work but in part also produced directly from excited α-DNBP or a short-lived intermediate, since the OH tautomer, as precursor of NH, is efficiently quenched at these concentrations of C211. The generation of NH via two parallel routes was previously observed in pure crystals,[10] and our results demonstrate an analogous behavior in liquid solutions.

The decay of NH by PT to the cage occurs with a rate that is proportional to the concentration of C211. The bimolecular rate constant of this reaction is $(2.5 \pm 1) \times 10^7$ s^{-1} M^{-1}. This reaction rate is smaller than the collision rate by more than 2 orders of magnitude and is thus clearly not diffusion limited.

The decay of the anion is due to PT from the cage to the anion, which regenerates the ground state CH_2 tautomer. The observation that this decay depends upon the concentration of C211 is somewhat unexpected, but can be rationalized by the presence of traces of other proton donors (e.g. H_2O) in the solution. PT from these impurities contributes to the anion decay. Deviations of the measured kinetic behavior at 1×10^{-3} M of [2.1.1] cryptand from the expected hyperbolic decay support this hypothesis. At higher concentrations of C211 these potential proton donors are deprotonated so that the protonation of the anion occurs only by deprotonation of the cryptand with a correspondingly lower rate. The observed decay follows indeed more closely the hyperbolic law, (1).

To evaluate the bimolecular rate constant of PT from the protonated cage to the anion, knowledge of the molar extinction coefficient of the anion is required. Taking the value of $\epsilon_{AN} = 1400$ M^{-1} cm^{-1}, measured for a chemically prepared anion of α-DNBP in a methanol solution of KOH,[14] and the effective path length of 0.25 cm, this rate constant is about 2×10^5 s^{-1} M^{-1}. This value is smaller by more than 4 orders of magnitude than the collision rate. This very low reaction rate demonstrates the stabilization of the proton in the cage and may be attributed to the special structural features of the resulting endo proton cryptate (see Scheme 1) and the structural changes accompanying its formation (see also above).

The observation, in the presence of a strong base, of a photoinduced anion of α-DNBP is in agreement with the results obtained for many other *ortho*-nitrobenzyl derivatives in which the photochromic reaction results in an equilibrium between the aci-nitro structure and its anion, displaced toward the anion in basic media.[15,16] In toluene solution, however, the anion should be very unstable and decay rapidly by recombination with the proton. This behavior is indeed observed with TEA as proton acceptor, where the decay of the anion, generated by deprotonation of OH, occurs on a time scale of $<10^{-5}$ s and is faster than the decay of NH so that a reasonable data analysis is prevented. Only a lower limit of the corresponding bimolecular rate constant can be given. This lower limit of 7×10^9 s^{-1} M^{-1} is higher by a factor of 3×10^4 than the corresponding rate obtained for the [2.1.1] cryptand, illustrating the special behavior of the latter.

V. Conclusion

We have shown here the feasibility of using C211 as a stabilized proton acceptor in a photoinduced PT reaction. The protonation of the cage clearly depends on the driving force (difference of pH), as shown by the differences in the rates of PT to the cage from OH and NH. When the cage will be chemically linked to the proton donor, the rate of PT is no longer diffusion limited. It remains to be established for such combinations if the acidity of the proton donor in the initially excited singlet state is sufficient to make the rate of PT higher than the deactivation rate of this state by other processes or if longer lived intermediate tautomers will always be required, such as provided by the OH tautomer in the case of α-DNBP, studied here. Our measurements do indicate that the retardation of the reverse PT reaction, that is the deprotonation of the cage, is sufficient to envision applications in the design of photochromic PT systems. Irrespective of these "engineering" aspects, the use of the cryptand in the present work has made it possible to establish reaction pathways for α-DNBP in solution by intercepting the intermediate OH tautomer on a fast time scale, such simplifying the disentanglement of the complex overlapping spectra. Finally, this study also demonstrates that suitably designed components allow control of proton transfer processes, a feature of crucial importance for the development of molecular protonic devices.[1]

Acknowledgment. Preliminary experiments and helpful advice from Y. Eichen and Z. Pikramenou are gratefully acknowledged. This work was supported by the EC ESPRIT Program (PROTIOS - 7238).

References and Notes

(1) Lehn, J.-M. *Supramolecular Chemistry - Concepts and Perspectives*; VCH: Weinheim, Germany, Chapter 8, 1995.

(2) Cheney, J.; Lehn, J.-M. *J. Chem. Soc., Chem. Commun.* **1972**, 487. Cheney, J.; Kintzinger, J.-P.; Lehn, J.-M. *Nouv. J. Chim.* **1978**, *2*, 411. Smith, P. B.; Dye, J. L.; Cheney, J.; Lehn, J.-M. *J. Am. Chem. Soc.* **1981**, *103*, 6044.

(3) Micheloni, M. *J. Coord. Chem.* **1988**, *18*, 3.

(4) Cox, B. G.; Murray-Rust, J.; Murray-Rust, P.; van Truong, N.; Schneider, H. *J. Chem. Soc., Chem. Commun* **1982**, 377. Luger, P.; Buschmann, J.; Knöchel, A.; Tiemann, O.; Patz, M. *Acta Crystallogr.* **1991**, *C47*, 1860, see also: Brügge, H. J.; Carboo, D.; von Deuten, D.; Knöchel, A.; Kopf, J.; Dreissing, W. *J. Am. Chem. Soc.* **1986**, *108*, 107.

(5) (a) Cox, B. G.; Knop, D.; Schneider, H. *J. Am. Chem. Soc.* **1978**, *100*, 6002. (b) Kjaer, A. M.; Soerensen, P. E., Ulstrup, J. *J. Chem. Soc., Chem. Commun.* **1979**, 965.

(6) Klemm, E.; Klemm, D.; Graness, A.; Kleinschmidt, J. *Chem. Phys. Lett.* **1978**, *55*, 113. Klemm, D.; Klemm, E.; Graness, A.; Kleinschmidt, J. *Z. Phys. Chem.* **1979**, *260*, 555. Klemm, D.; Klemm, E. *J. Prakt. Chem.* **1979**, *321*, 404.

(7) Takahashi, H.; Kobayashi, Y.; Kaneko, N.; Igarashi, T.; Yagi, I. *J. Raman Spectrosc.* **1982**, *12*, 125.

(8) Corval, A.; Kuldová, K.; Eichen, Y.; Pikramenou, Z.; Lehn, J.-M.; Trommsdorff, H. P. *J. Phys. Chem.* **1996**, *100*, 19315.

(9) Sixl, H.; Warta, R. *Chem. Phys.* **1985**, *94*, 147.

(10) Casalegno, R.; Corval, A.; Kuldová, K.; Ziane, O.; Trommsdorff, H. P. *J. Lumin.* **1997**, *72−74*, 78.

(11) Kimura, H.; Sakata, K.; Takahashi, H. *J. Mol. Struct.* **1993**, *1−4*, 293.

(12) Kuldová, K. Ph.D. Thesis, 1997, Grenoble.

(13) Mosher, H. S.; Hardwick, E. R.; Ben-Hur, D.; *J. Chem. Phys.* **1962**, *37*, 904.

(14) Pikramenou, Z. Private communication.

(15) Margerum, J. D.; Miller, L. J.; Saito, E.; Brown, M. S.; Mosher, H. S.; Hardwick, R. *J. Phys. Chem.* **1962**, *66*, 2434.

(16) Atherton, S. J.; Craig, B. B. *Chem. Phys. Lett.* **1986**, *127*, 7.